DAMAGE IN DOMAINS AND INTERFACES: A COUPLED PREDICTIVE THEORY

Francesco Freddi and Michel Frémond

msp

DAMAGE IN DOMAINS AND INTERFACES: A COUPLED PREDICTIVE THEORY

FRANCESCO FREDDI AND MICHEL FRÉMOND

In this study, we propose a model coupling damage of domains and damage of interfaces. A predictive theory of continuum damage mechanics is developed within the framework of the principle of virtual power. Because damage results from microscopic motions, the power of these microscopic motions is included in the power of the internal forces. The power of the internal forces we choose depends on the damage velocity and on its gradient to take into account local interactions. An interaction between the domain damage and the damage along the interface is introduced. To overcome the insensitivity of the local interface model to elongation, nonlocal elongation has been considered as a source of damage. Representative numerical examples confirm that our proposed model can be used to describe various damage phenomena in agreement with experiments.

1. Introduction

Mechanical degradation of quasibrittle materials is usually traced back to development of micro-cracking and microvoids. Continuum damage mechanics based upon general principles which govern the evolution of the variables representative of the material state is an effective tool for analysis of these behaviors, [Lemaitre 1992; Stumpf and Hackl 2003; Mosconi 2006]. In particular, isotropic damage formulations are extensively employed in the literature because of their simplicity, efficiency and adequacy for many practical applications [Voyaiadjis et al. 1998; Lemaitre and Desmorat 2005]. Damage theory has been used successfully to describe adhesion of solids [Borino and Failla 2005; Alfano and Crisfield 2001; Zou et al. 2003]. In fact, the interface regions between materials fundamentally governs the strength and stability of structural elements [Truong Dinh Tien 1990]. Moreover, structural collapse in composite structures is often caused by the appearance and evolution of different damage phenomena in a narrow region near the interface [Yao et al. 2005; Aimi et al. 2007; Freddi and Savoia 2006; Gonzalez et al. 2005].

The practical problem is to determine whether the design of a future structure forbids any failure by surface or volume damage under service loads. Predictive theories must account for these physical results, including short-term behaviour.

The present work deals with the structural response of quasibrittle domains, for instance pieces of concrete glued on one another. We take into account both volume and interface damaging behaviors and their interactions. As a starting point, we used two damage models proposed in [Frémond and Nedjar 1996; Frémond 2001] for the description of domain and interface behaviour. These models are based on adaptation of the principle of virtual power. In particular, we assume that damage results from microscopic motions, and include the power of these motions in the principle of virtual power. This power contribution is assumed to depend on the strain rate (displacement discontinuity for the interface), the

rate of damage and the damage gradient (damage discontinuity for the interface). The damage gradient is introduced to account for the local interaction of the damage at a material point on the damage of its neighborhood. Correspondingly, we also introduce two new quantities: the internal work of damage and the flux vector of internal work of damage (adhesion energy and energy flux vector of the contact surface).

On the contact surface there are local damage interactions between damage at a point and damage in its neighborhood. Thus there is interaction within the glue as well as interaction between the glue and the two concrete pieces. These interactions are defined usch that their virtual power involves appropriate kinematic quantities. For instance, experiments show that elongation may have damaging effects. In this setting, an elongation is a variation of the distance between two distinct points belonging to the contact surface. This is a nonlocal quantity which introduces nonlocal contributions in the theory.

The principle of virtual power leads to three sets of equations of motion; the first is the classical equation of motion and the other two are nonstandard fields representative of the domains and evolution of interface damage.

The constitutive laws we adopt permit us to control the energy dissipated during degradation and separation of solids so as to avoid stiffness recovery and cohesive state restoration. Suitable free energies let us express nonstandard internal forces conjugated to the damage rate and the gradient damage rate. We then introduce pseudo-potentials of dissipation to characterize the damage evolution. The internal constraints on the values of damage quantities and on their velocities are taken into account explicitly in the expressions of the free energy and of the pseudo-potential.

The domain model derived from this formulation is not affected by mesh sensitivity. In fact, the damage model for the domains overcomes the well-known problem of mesh dependence: a boundary value problem that governs the evolution of the damage variable instead of the usual local constitutive law. Moreover, impenetrability between domains is included in the constitutive laws, thus avoiding the introduction of interface parameters for penalty stiffness, parameters which can create numerical problems, such as spurious traction oscillations [Alfano and Crisfield 2001]. Numerical simulations are proposed which correctly determine whether the zone affected by damage is the interface or a narrow region inside the domains. Specific cases of two concrete elements glued together are considered and a FRP-concrete delamination test is performed. In some cases, we compare the experimental results quantitatively and qualitatively to computations.

Several studies have considered the two models separately. For the domain model the behaviour of concrete structures is correctly predicted in [Frémond and Nedjar 1996] and [Frémond 2001]. Recently, an extension to elastoplastic-damage model was proposed in [Nedjar 2001] and numerical aspects were investigated in [Nedjar 2002] and [Ireman 2005].

Moreover, some mathematical results are reported in [Frémond et al. 1998]. Dynamic processes of adhesive contact with a deformable foundation are considered in [Truong Dinh Tien 1990; Chau et al. 2004], where the rate of bonding field is assumed to be reversible and irreversible. [Bonetti et al. 2005] obtained the global existence and uniqueness results for two solids glued together and results for local existence for a damage model in elastic materials were reported in [Bonetti and Schimperna 2004; Bonetti et al. 2006]. In addition, a model coupling adhesion, friction and unilateral contact is considered in [Raous et al. 1999] and [Raous and Monerie 2002].

2. Physical capacities, potentialities and limits of the model

Gluing of structural elements, an attractive assembly method in civil engineering, must always be evaluated with respect to both short- and long-term behavior. In the short term, we must answer the question: Is the structure designed so that the glued connections and the mechanical elements are strong enough to support the service loads? Over the long term the question becomes: is the operating structure still solid, or must it be strengthened?

The predictive theory we present answers the first question by determining the service load. Once the service load is known, it is possible to predict if the design is such that the future structure will be free of volume or surface damage which would lead to immediate collapse. The examples of Section 7 clearly show that the computer program resulting from our model is efficient and versatile enough to deal with very different structures made of glued parts. Beyond the damage of glued connections, the theory also predicts coupling with the volume damage which can also endanger structures.

The theory is sparing of parameters (three for each material): a cohesion parameter, an extension parameter and a viscosity parameter. We think this is the minimum number of parameters to correctly describe damaging phenomena and answer questions about the damage, such as:

(a) Does damage appear (cohesion parameter)?

(b) Does the damage extend or remain concentrated in thin zones (extension parameter)?

(c) Does the damage evolve slowly or rapidly (viscosity parameter)?

For the glue, we have used the three parameters above and three more extension parameters to describe nonlocal interactions within the glue and the interaction of the glue with its neighboring materials

For short-term behavior, we have established the capabilities of the predictive theory. Its limitations are mainly mechanical and are due to the elastic-damaging constitutive law. Let us also note that for the surface, the constitutive laws which involve nonlocal actions are much richer than needed for some practical applications.

For long-term behavior, aging theory must be added together with rules to determine the related parameters. The predictive theory seems a good starting point, and some results are already available [Bruneaux 2004].

3. State quantities and quantities describing the evolution

In this section we introduce the state quantities E, and the quantities δE describing the evolution or development of damage. Let us consider a system made of two domains Ω_i, $i = 1, 2$, in the undistorted natural reference configuration subjected to mixed boundary conditions and connected by an adhesive interface $\Gamma_s = \partial\Omega_1 \cap \partial\Omega_2$. An example is a system of two pieces of concrete glued on one another.

For the sake of simplicity, we neglect the thermal effects, do not take the temperature into account, and limit our analysis to small perturbation theory. Note that the equations of motion reported in Section 4 are valid without this restriction.

For each domain Ω_i, the state quantities are the macroscopic damage quantity $\beta_i(\vec{x}, t)$, its gradient $\operatorname{grad}\beta_i(\vec{x}, t)$ and deformation $\varepsilon_i(\vec{x}, t)$. The values of $\beta_i(\vec{x}, t)$ are between 0 and 1, where 1 represents the undamaged state and 0 the completely damaged one. Damage quantity β_i may be understood as the volume fraction of active links or of undamaged material. The gradient of $\beta_i(\vec{x}, t)$ accounts for local

interactions of the damage at a point on damage of its neigbourhood. Recall that the deformation $\varepsilon_i(\vec{x}, t)$ accounts for the local interaction of the displacement at a point on displacement of its neighborhood.

The quantities which describe the evolution in each domain Ω_i are the velocities of the state quantities. The velocities $d\beta/dt$ account for the microscopic velocities at the macroscopic level.

The state quantities on the contact surface $\partial\Omega_1 \cap \partial\Omega_2$ involve quantities which describe the evolution of the surface, and quantities which describe the macroscopic and microscopic interactions between domains and surface. The quantities which describe the surface evolution, for instance the glue evolution, are the surface or glue damage quantity, and its surface gradient, $\beta_s(\vec{x}, t)$, and $\text{grad}_s \beta_s(\vec{x}, t)$ taking into account the local damage interaction in the surface or in the glue. The macroscopic interactions are described by the gap as is usual in contact mechanics, and also by the elongation, a new nonlocal state quantity which describes the variation of the distance of two different points of the surface. Microscopic interactions are also described by the traces of the domain damage quantities.

The gap $\vec{u}_2(\vec{x}) - \vec{u}_1(\vec{x})$ is the difference between two small displacements $\vec{u}_i$ at the same point $\vec{x}$ of the surface. Note that even if the gap is 0, the displacements which are not equal at two different points of the surface would produce a notable damaging action. To account for this property, we introduce the elongation

$$g(\vec{x}, \vec{y}) = 2(\vec{y} - \vec{x}) \cdot (\vec{u}_2(\vec{y}) - \vec{u}_1(\vec{x})) \,.$$

It describes the evolution of the distance between two different points, $\vec{x}$ and $\vec{y}$, and it may be different from 0 if the gap is 0.

The quantities describing the evolution of the contact surface are the velocities of the state quantities. The velocity of the elongation is

$$D_{1,2}(\vec{U}_1, \vec{U}_2)(\vec{x}, \vec{y}) = 2(\vec{y} - \vec{x}) \cdot (\vec{U}_2(\vec{y}) - \vec{U}_1(\vec{x})).$$

where $\vec{U}_i = d\vec{u}_i/dt$ are the macroscopic velocities.

Let us note that this velocity is 0 in any rigid system velocity, that is, a set of velocities which do not change the form of the system. It is easy to check that rigid system velocities satisfy

$$\vec{U}_1(\vec{x}) = \vec{A} + \vec{B} \times x,$$

$$\vec{U}_2(\vec{x}) = \vec{A} + \vec{B} \times \vec{x},$$

$$\frac{d\beta_1}{dt} = \frac{d\beta_2}{dt} = \frac{d\beta_s}{dt} = 0.$$

These rigid velocities do not change the form of the system because the gap does not change on the contact surface. Moreover, since the damage velocities are 0, the microscopic velocities which are responsible for their evolutions are 0.

Remark 1. The velocity of the elongation is the time derivative of the square of the distance of two points

$$D_{1,2}(\vec{U}_1, \vec{U}_2)(\vec{x}, \vec{y}) = 2(\vec{y} - \vec{x}) \cdot (\vec{U}_2(\vec{y}) - \vec{U}_1(\vec{x})) = \frac{d}{dt}(\vec{y} - \vec{x})^2.$$

We find that within the small deformation assumption, the elongation $g(\vec{y}, \vec{x})$ is the variation of the square of the distance of the two points. The physical properties of the internal force associated with the elongation may be understood with this property.

To sum up, the state quantities E and the quantities describing the evolution are, in Ω_1 and in Ω_2,

$$E_1 = \{\varepsilon_1, \beta_1, \text{grad } \beta_1\}, \quad \delta E_1 = \left\{\frac{d\varepsilon_1}{dt}, \frac{d\beta_1}{dt}, \text{grad } \frac{d\beta_1}{dt}\right\},$$

$$E_2 = \{\varepsilon_2, \beta_2, \text{grad } \beta_2\}, \quad \delta E_2 = \left\{\frac{d\varepsilon_2}{dt}, \frac{d\beta_2}{dt}, \text{grad } \frac{d\beta_2}{dt}\right\},$$

where $d\varepsilon_i/dt$ are the classical strain rates.

On the contact surface $\partial\Omega_1 \cap \partial\Omega_2$

$$E_s = \{\vec{u}_2 - \vec{u}_1, \beta_s, \text{grad}_s\, \beta_s, \beta_1 - \beta_s, \beta_2 - \beta_s\},$$

$$E_{s,1,2} = \{g(\vec{x}, \vec{y}) = 2(\vec{y} - \vec{x}) \cdot (\vec{u}_2(\vec{y}) - \vec{u}_1(\vec{x})), \beta_s(\vec{x}), \beta_s(\vec{y})\},$$

$$\delta E_s = \left\{\vec{U}_2 - \vec{U}_1, \frac{d\beta_s}{dt}, \text{grad}_s\, \frac{d\beta_s}{dt}, \frac{d\beta_1}{dt} - \frac{d\beta_s}{dt}, \frac{d\beta_2}{dt} - \frac{d\beta_s}{dt}\right\},$$

$$\delta E_{s,1,2}(\vec{x}, \vec{y}) = \left\{D_{1,2}(\vec{U}_1, \vec{U}_2)(\vec{x}, \vec{y}), \frac{d\beta_s}{dt}(\vec{x}), \frac{d\beta_s}{dt}(\vec{y})\right\},$$

where $\beta_i - \beta_s$ is the discrete analog of the gradient.

4. Equations of motion

The equations of motion result from the principle of virtual power which involves the powers of the internal forces, the exterior forces, and the acceleration forces and which yield the introduction of new internal forces which describe the evolution and interaction of damage variables.

4.1. *Virtual power of the internal forces.* Both volume damage and surface damage result from microscopic motions whose power is taken into account in the power of the internal forces. We have chosen the velocities $d\beta/dt$ to account for the microscopic velocities at the macroscopic level. Assuming $\vec{V} = (\vec{V}_1, \vec{V}_2)$ and $\gamma = (\gamma_1, \gamma_2, \gamma_s)$ to be macroscopic and microscopic virtual velocities, the virtual power of the internal forces, which is a linear function of the virtual velocities, is chosen to be

$$\mathscr{P}_{int} = -\int_{\Omega_1} \sigma_1 : D(\vec{V}_1)d\Omega - \int_{\Omega_1} B_1\gamma_1 + \vec{H}_1 \cdot \text{grad } \gamma_1 d\Omega$$

$$-\int_{\Omega_2} \sigma_2 : D(\vec{V}_2)d\Omega - \int_{\Omega_2} B_2\gamma_2 + \vec{H}_2 \cdot \text{grad } \gamma_2 d\Omega$$

$$-\int_{\partial\Omega_1 \cap \partial\Omega_2} \vec{R}(\vec{V}_2 - \vec{V}_1)d\Gamma - \int_{\partial\Omega_1 \cap \partial\Omega_2} B_s\gamma_s + \vec{H}_s \cdot \text{grad}_s\, \gamma_s + B_{1,s}(\gamma_1 - \gamma_s) + B_{2,s}(\gamma_2 - \gamma_s)d\Gamma$$

$$+\int_{\partial\Omega_1 \cap \partial\Omega_2} \int_{\partial\Omega_1 \cap \partial\Omega_2} M(\vec{x}, \vec{y})D_{1,2}(\vec{V}_1, \vec{V}_2)(\vec{x}, \vec{y})d\Gamma(\vec{x})d\Gamma(\vec{y})$$

$$+\int_{\partial\Omega_1 \cap \partial\Omega_2} \int_{\partial\Omega_1 \cap \partial\Omega_2} B_{s,1}(\vec{x}, \vec{y})\gamma_s(\vec{x}) + B_{s,2}(\vec{x}, \vec{y})\gamma_s(\vec{y})d\Gamma(\vec{x})d\Gamma(\vec{y}),$$

where

$$(D(\vec{V}))_{i,j} = \frac{1}{2}(\frac{\partial V_i}{\partial x_j} + \frac{\partial V_j}{\partial x_i}) = \frac{1}{2}(V_{i,j} + V_{j,i})$$

are the classical strain rates. The different quantities which contribute to the power of the internal forces are products of kinematic quantities by internal forces. Kinematic quantities are those which intervene in the motion we intend to describe. Their choice is of paramount importance to the predictive capability of the theory. They are chosen following the experimental phenomena of volume and surface deformations together with volume and surface damage, that is, microvoiding and microcracking. Thus the model includes quantities with surface and volume densities which depend on the quantities we have chosen to describe the evolutions or the deformations of the system. Some are classical and others are new. Also, most are local but a few are nonlocal because there is a nonlocal kinematic quantity. Let us comment on the different power densities:

- The usual strain rate D introduces the stress σ.

- The damage velocity, $d\beta/dt$ is a scalar, thus the associated internal force is also a scalar, B. It is a mechanical work, specifically, the internal damage work which is responsible for the evolution of the damage in the volume and in the surface.

- The gradient of the damage velocity, $\text{grad}(d\beta/dt)$ is a vector, thus the internal force is a vector, $\vec{H}$. It is a work flux vector which is responsible for the interaction of the damage at a point on the damage of its neighborhood. Its physical meaning is to be given by the boundary condition of the equation of motion just as the physical meaning of the stress is given by the boundary condition of the equation of motion.

- The gap velocity $\vec{U}_2 - \vec{U}_1$ on the contact surface introduces the classical macroscopic interaction force $\vec{R}$.

- The difference between the damage velocities $d\beta_i/dt - d\beta_s/dt$ introduces a damage work flux on the surface $B_{i,s}$, which describes the influence of the volume damage on the surface damage.

- The nonlocal elongation velocity, $D_{1,2}(\vec{U}_1, \vec{U}_2)(\vec{x}, \vec{y})$ introduces a nonlocal scalar $M(\vec{x}, \vec{y})$ internal force. It describes the effects of the elongation, and results in the equations of motion as a classical force. The interaction macroscopic mechanical force has a nonlocal part and a classical local part, the force $\vec{R}$ (see Equation (5)). Since we are going to assume the internal force $M(\vec{x}, \vec{y})$ depending on the surface damage β_s, it is wise to add an extra nonlocal power depending on damage velocity $d\beta_s/dt$. It describes the effect of damage at point $\vec{x}$ on damage at point $\vec{y}$. The internal forces $B_{s,i}(\vec{x}, \vec{y})$ have the same effect than M: they introduce a nonlocal internal source of damage work. The microscopic mechanical force has a nonlocal part and three local parts, B_s due to the glue and the two $B_{i,s}$ due to the interactions which the volumes (see Equation (7) below).

Note that even if the internal forces are numerous and some are unusual, they are all simple and precisely chosen to take into account a particular aspect of the coupling of volume and surface, and of the microscopic and macroscopic evolution of the system.

4.2. *Virtual power of the exterior forces.* We assume no exterior microscopic surfacic or volumic source of damage, such as radiative, electrical or chemical damaging actions. Thus the power does not depend

on γ, and we have

$$\mathscr{P}_{ext} = \int_{\Omega_1} \vec{f}_1 \vec{V}_1 d\Omega + \int_{\partial\Omega_1 \setminus (\partial\Omega_1 \cap \partial\Omega_2)} \vec{g}_1 \vec{V}_1 d\Gamma + \int_{\Omega_2} \vec{f}_2 \vec{V}_2 d\Omega + \int_{\partial\Omega_2 \setminus (\partial\Omega_1 \cap \partial\Omega_2)} \vec{g}_2 \vec{V}_2 d\Gamma,$$

where the $\vec{f}$ and $\vec{g}$ are the body and surface exterior forces.

4.3. *Virtual power of the acceleration forces.* For the sake of simplicity, we assume a quasistatic problem. Thus

$$\mathscr{P}_{acc} = 0.$$

4.4. *The principle of virtual power and the equations of motion.* The principle of virtual power

$$\mathscr{P}_{acc} = \mathscr{P}_{int} + \mathscr{P}_{ext}, \quad \text{for all } \vec{V}_1, \vec{V}_2, \gamma_1, \gamma_2, \gamma_s,$$

gives three sets of equations of motion. By choosing convenient virtual velocities, we obtain

$$\text{div } \sigma_i + \vec{f}_i = 0, \quad \text{in } \Omega_i, \tag{1}$$

$$-B_i + \text{div } \vec{H}_i = 0, \quad \text{in } \Omega_i, \tag{2}$$

$$\sigma_i \vec{N}_i = \vec{g}_i, \quad \text{in } \partial\Omega_i \setminus (\partial\Omega_1 \cap \partial\Omega_2), \tag{3}$$

$$\vec{H}_i \vec{N}_i = 0, \quad \text{in } \partial\Omega_i \setminus (\partial\Omega_1 \cap \partial\Omega_2), \tag{4}$$

where the $\vec{N}_i$ are the outward normal to the Ω_i. Equations (1)–(4) are the volume equations of motion accounting for macroscopic and microscopic effects. The equation of motion (3) gives the physical meaning of the stress tensor. In the same way, the equation of motion (4) gives the physical meaning of vector $\vec{H}$: its scalar product with vector $\vec{N}$ is the amount of work which is provided to the domain with exterior normal $\vec{N}$ by microscopic motions. These microscopic motions may be due either to macroscopic deformations (as in the examples given below), or to radiative, electrical, chemical, and optical actions.

On surface $\partial\Omega_1 \cap \Omega_2$, the boundary conditions for the volume equations of motion (1) and (2), as well as the surface equation of motion, involve nonlocal forces. For the volume equations of motion (1), the boundary conditions are

$$\sigma_1 \vec{N}_1(\vec{x}) = \vec{R}(\vec{x}) + \int_{\partial\Omega_1 \cap \partial\Omega_2} 2(\vec{x} - \vec{y}) M(\vec{x}, \vec{y}) d\Gamma(\vec{y}), \quad \vec{x} \in \partial\Omega_1 \cap \partial\Omega_2,$$

$$\sigma_2 \vec{N}_2(\vec{y}) = -\vec{R}(\vec{y}) + \int_{\partial\Omega_1 \cap \partial\Omega_2} 2(\vec{y} - \vec{x}) M(\vec{x}, \vec{y}) d\Gamma(\vec{x}), \quad \vec{y} \in \partial\Omega_1 \cap \partial\Omega_2. \tag{5}$$

As already mentioned, the stress $\sigma_i \vec{N}_i$ on the contact surface has a local part $\vec{R}$ and a nonlocal part

$$\int_{\partial\Omega_1 \cap \partial\Omega_2} (-1)^i \, 2 \, (\vec{y} - \vec{x}) M(\vec{x}, \vec{y}) d\Gamma(\vec{x}).$$

The boundary conditions for the equation of motions (2) in $\partial\Omega_1 \cap \partial\Omega_2$ are

$$\vec{H}_1 \vec{N}_1 = -B_{1,s}, \qquad \vec{H}_2 \vec{N}_2 = -B_{2,s}, \tag{6}$$

and a surface equation of motion with a boundary condition on the boundary of the contact surface $\partial(\partial\Omega_1 \cap \partial\Omega_2)$,

$$-B_s(\vec{x})+\text{div}_s \, \vec{H}_s(\vec{x})+B_{1,s}(\vec{x})+B_{2,s}(\vec{x})-\int_{\partial\Omega_1\cap\partial\Omega_2} B_{s,1}(\vec{x},\vec{y})+B_{s,2}(\vec{y},\vec{x})d\Gamma(\vec{y})=0, \quad \text{in } \partial\Omega_1\cap\partial\Omega_2,$$
$$\vec{H}_s\vec{n}_s = 0, \quad \text{in } \partial(\partial\Omega_1 \cap \partial\Omega_2), \tag{7}$$

where div_s is the surface divergence and $\vec{n}_s$ is normal vector to the boundary $\partial(\partial\Omega_1 \cap \Omega_2)$. As already mentioned, the internal source of damage on the contact surface has three local parts $-B_s(\vec{x})$ due to the glue and $B_{1,s}(\vec{x})$, $B_{2,s}(\vec{x})$ due to the two neighboring volumes, and a nonlocal part

$$\int_{\partial\Omega_1\cap\partial\Omega_2} B_{s,1}(\vec{x},\vec{y}) + B_{s,2}(\vec{y},\vec{x})d\Gamma(\vec{y}).$$

Of course, the opposite of the damage work $B_{1,s}(\vec{x})$ and $B_{2,s}(\vec{x})$ which are provided to the glue by the two neighboring volumes, are provided by the glue to the volumes by Equations (6) and (7).

Constitutive laws are needed for the numerous interior forces. As usual, we choose to define them with free energies Ψ depending on state quantities E and pseudo-potential of dissipation Φ depending on velocities δE.

5. The constitutive laws

Since the thermal phenomena are not taken into account, the second law of thermodynamics for the domains and the interface are [Frémond 2001]

$$\frac{d\Psi_i}{dt}(E_i) \leq \sigma_i D\left(\vec{U}_1\right) + B_i \frac{d\beta_i}{dt} + \vec{H}_i \, \text{grad} \, \frac{d\beta_i}{dt}, \quad \text{in } \Omega_i, \tag{8}$$

$$\frac{d\Psi_s}{dt}(E_s) \leq \vec{R}\left(\vec{U}_2 - \vec{U}_1\right) + B_s \frac{d\beta_s}{dt} + \vec{H}_s \, \text{grad}_s \, \frac{d\beta_s}{dt}$$
$$+ B_{1,s}\left(\frac{d\beta_1}{dt} - \frac{d\beta_s}{dt}\right) + B_{2,s}\left(\frac{d\beta_2}{dt} - \frac{d\beta_s}{dt}\right), \quad \text{in } \partial\Omega_1 \cap \partial\Omega_2, \tag{9}$$

$$\frac{d\Psi_{s,1,2}}{dt}\left(E_{s,1,2}\right)(\vec{x},\vec{y}) \leq -M(\vec{x},\vec{y})D_{1,2}\left(\vec{U}_1,\vec{U}_2\right)(\vec{x},\vec{y}),$$
$$- B_{1,s}(\vec{x},\vec{y})\frac{d\beta_s}{dt}(\vec{x}) - B_{2,s}(\vec{x},\vec{y})\frac{d\beta_s}{dt}(\vec{y}), \quad \text{in } (\partial\Omega_1 \cap \partial\Omega_2) \times (\partial\Omega_1 \cap \partial\Omega_2). \tag{10}$$

We use Equations (8)–(10) to define the constitutive laws with pseudo-potential of dissipation. The $+$ or $-$ sign appearing in the constitutive laws results from the $+$ or $-$ sign in the right sides of the inequalities, and right sides are the opposite of the densities of the virtual powers.

The free energy and pseudo-potential of dissipation of the domains are, respectively,

$$\Psi_i(E_i) = \Psi_i\left(\varepsilon_i, \beta_i, \text{grad } \beta_i\right) \in w_i(1 - \beta_i) + \frac{k_i}{2} \left(\text{grad } \beta_i\right)^2 + I(\beta_i) + \frac{\beta_i}{2} \left\{\lambda_i \left(\text{tr } \varepsilon_i\right)^2 + 2\mu_i \varepsilon_i : \varepsilon_i\right\},$$

$$\Phi_i(\delta E_i) = \Phi_i\left(\frac{d\beta_i}{dt}\right) = \frac{c_i}{2}\left(\frac{d\beta_i}{dt}\right)^2 + I_-\left(\frac{d\beta_i}{dt}\right),$$

where λ_i and μ_i are the Lamé parameters. The quantities w_i are initial damage thresholds expressed in terms of volumetric energies. They are equivalent to the initial thresholds expressed in terms of damage forces or stresses [Lemaitre 1992; Voyaiadjis et al. 1998; Lemaitre and Desmorat 2005]. The quantities c_i are the viscosity parameters of damage and k_i measure the local influences of a material point on its neighborhood. The c_i quantities control the velocity of the phenomena. If they are large, damage evolution is slow and if they are small, damage evolution is very fast. The values of c_i can be measured with experiments performed at different velocities. The extension parameters k_i control the size of the transition zone between sound material and damaged material. If the k_i are large, damage is diffuse and spread in the whole domain. If the k_i are small, the damage is concentrated in thin zones which may represent fractures. The values of k_i can be measured with structure experiments, but not with sample experiments where the state quantities are homogeneous.

The functions I and I_- are the indicator functions of the intervals $[0, 1]$, $(I(\gamma) = 0$, if $0 \le \gamma \le 1$, and $I(\gamma) = +\infty$, if $\gamma \notin [0, 1])$, and of $[-\infty, 0] = \mathbb{R}^-$, $(I_-(\gamma) = 0$, if $\gamma \le 0$ and $I_-(\gamma) = +\infty$, if $\gamma > 0)$ (see [Moreau 1966]).

The free energies and pseudo-potentials are the most simple energies coupling elasticity and damage. They give the constitutive laws

$$\sigma_i = \frac{\partial \Psi_i}{\partial \varepsilon_i} = \beta_i \left\{\lambda_i \text{ tr } \varepsilon_i \mathbf{1} + 2\mu_i \varepsilon_i\right\},$$

$$B_i = \frac{\partial \Psi_i}{\partial \beta_i} + \frac{\partial \Phi_i}{\partial (d\beta_i/dt)}$$

$$\in -w_i + \frac{1}{2}\left\{\lambda_i \left(\text{tr } \varepsilon_i\right)^2 + 2\mu_i \varepsilon_i : \varepsilon_i\right\} + \partial I(\beta_i) + c_i\left(\frac{d\beta_i}{dt}\right) + \partial I_-\left(\frac{d\beta_i}{dt}\right),$$

$$\vec{H}_i = \frac{\partial \Psi_i}{\partial (\text{grad } \beta_i)} = k_i \text{ grad } \beta_i.$$

where $\mathbf{1}$ is the identity matrix.

In the previous formula, ∂I and ∂I_- are the subdifferential sets or the sets of the generalized derivatives of the indicator functions I, $(\partial I(\beta) = \{0\}$, if $0 < \beta < 1$; $\partial I(0) = \mathbb{R}^-$; $\partial I(1) = \mathbb{R}^+ = [0, +\infty[$; $\partial I(\beta) = \varnothing$, if $\beta \notin [0, 1])$ and I_-, $(\partial I_-(x) = \{0\}$, if $x < 0$ and $\partial I_-(0) = [0, +\infty[)$. These generalized derivatives are the reactions to the internal constraints $0 \le \beta_i \le 1$ and $d\beta_i/dt \le 0$. The latter internal constraint accounts for the irreversibility of damage. The reactions are different from 0 only for the extreme values of the inequalities.

The free energy and pseudo-potential of the glued contact surface are

$$\Psi_s(E_s) = \Psi_s\left(\vec{u}_2 - \vec{u}_1, \beta_s, \text{grad}_s\,\beta_s, \beta_1 - \beta_s, \beta_2 - \beta_s\right)$$

$$= w_s(1 - \beta_s) + \frac{k_s}{2}\left(\text{grad}_s\,\beta_s\right)^2 + I(\beta_s) + I_-\left((\vec{u}_2 - \vec{u}_1)\cdot\vec{N}_2\right)$$

$$+ \frac{\beta_s \hat{k}_s}{2}\,(\vec{u}_2 - \vec{u}_1)^2 + \frac{k_{s,1}}{2}\,(\beta_1 - \beta_s)^2 + \frac{k_{s,2}}{2}\,(\beta_2 - \beta_s)^2\,,$$

$$\Phi_s(\delta E_s) = \Phi_s(\frac{d\beta_s}{dt}) = \frac{c_s}{2}\left(\frac{d\beta_s}{dt}\right)^2 + I_-\left(\frac{d\beta_s}{dt}\right),$$

where k_s is the local surface extension or interaction coefficient, w_s the Dupré's energy accounting for the glue cohesion, c_s the viscosity of the adhesive evolution, $k_{s,1}$ and $k_{s,2}$ are the surface-volume interaction parameters, and $\hat{k}_s$ represents the rigidity of the bonds between the two solids. The function $I_-((\vec{u}_1 - \vec{u}_1)\cdot\vec{N}_2)$ takes into account the impenetrability of the two domains on their contact surface and function $I_-(d\beta_s/dt)$ implies irreversibility of damage.

The expressions of the free energy and pseudo-potential of dissipation are the simplest to give a model where damage is coupled with elasticity. They account for elastic, viscous and damage properties. The resulting constitutive laws are

$$\vec{R} = \frac{\partial\Psi_s}{\partial(\vec{u}_2 - \vec{u}_1)} \in \beta_s\hat{k}_s\,(\vec{u}_2 - \vec{u}_1) + \partial I_-\left((\vec{u}_2 - \vec{u}_1)\cdot\vec{N}_2\right)\vec{N}_2,$$

$$B_s = \frac{\partial\Psi_s}{\partial\beta_s} + \frac{\partial\Phi_s}{\partial(d\beta_s/dt)} \in -w_s + \frac{\hat{k}_s}{2}\,(\vec{u}_2 - \vec{u}_1)^2 + \partial I(\beta_s) + c_s\frac{d\beta_s}{dt} + \partial I_-\left(\frac{d\beta_s}{dt}\right),$$

$$\vec{H}_s = \frac{\partial\Psi_s}{\partial\left(\text{grad}_s\,\beta_s\right)} = k_s\,\text{grad}_s\,\beta_s,$$

$$B_{1,s} = \frac{\partial\Psi_s}{\partial(\beta_1 - \beta_s)} = k_{s,1}\,(\beta_1 - \beta_s)\,,$$

$$B_{2,s} = \frac{\partial\Psi_s}{\partial(\beta_2 - \beta_s)} = k_{s,2}\,(\beta_2 - \beta_s)\,.$$

The force $\partial I_-((\vec{u}_2 - \vec{u}_1)\cdot\vec{N}_2)\vec{N}_2$ is the impenetrability reaction. Note that it is active only when there is actually contact, that is, when $(\vec{u}_2 - \vec{u}_1)\cdot\vec{N}_2 = 0$.

The nonlocal free energy on the glued contact surface is

$$\Psi_{s,1,2}(E_{s,1,2}(\vec{x},\vec{y})) = \frac{k_{s,1,2}}{2}\,g^2(\vec{x},\vec{y})\,(\beta_s(\vec{x})\beta_s(\vec{y}))\exp(-\frac{|\vec{x} - \vec{y}|^2}{d^2}),$$

with

$$g(\vec{x},\vec{y}) = 2(\vec{y} - \vec{x})\cdot(\vec{u}_2(\vec{y}) - \vec{u}_1(\vec{x})).$$

The exponential function with distance d, describes the attenuation of nonlocal actions with distance $|\vec{x} - \vec{y}|$ between points $\vec{x}$ and $\vec{y}$. Assuming no dissipation with respect to $\delta E_{s,1,2}(\vec{x},\vec{y})$, we have the

constitutive law

$$-B_{s,1}(\vec{x}, \vec{y}) = \frac{\partial \Psi_{s,1,2}(E_{s,1,2}(\vec{x}, \vec{y}))}{\partial \beta_s(\vec{x})} = \frac{k_{s,1,2}}{2} g^2(\vec{x}, \vec{y}) \beta_s(\vec{y}) \exp\left(-\frac{|\vec{x} - \vec{y}|^2}{d^2}\right),$$

$$-B_{s,2}(\vec{x}, \vec{y}) = \frac{\partial \Psi_{s,1,2}(E_{s,1,2}(\vec{x}, \vec{y}))}{\partial \beta_s(\vec{y})} = \frac{k_{s,1,2}}{2} g^2(\vec{x}, \vec{y}) \beta_s(\vec{x}) \exp\left(-\frac{|\vec{x} - \vec{y}|^2}{d^2}\right),$$

$$-M(\vec{x}, \vec{y}) = \frac{\partial \Psi_{s,1,2}(E_{s,1,2}(\vec{x}, \vec{y}))}{\partial g(\vec{x}, \vec{y})} = k_{s,1,2} g(\vec{x}, \vec{y})(\beta_s(\vec{x})\beta_s(\vec{y})) \exp\left(-\frac{|\vec{x} - \vec{y}|^2}{d^2}\right).$$

The state quantities we use have dimension. The time and length scales related to the classical quantities are those of solids mechanics, in particular, of civil engineering. The new length scales are related to the gradient of damage, which corresponds to the size of the influence zone of damage (a few centimeters in our examples), and to the effect of damage elongation (on the order of millimeters in our examples). The first length scale is already known. To measure it, structure experiments have to be performed; in our case we used four point bending experiments. The second length scale has also been estimated with the four point bending experiments. Systematic research is under way at the Laboratoire Central des Ponts et Chaussées to estimate the amplitude of the variations of these parameters related to the durability of glued structures. Moreover, the parameters c_i may be seen as the characteristic times of the processes. They can be identified by performing experiments at different loading velocities, specifically, small velocities to remain in a quasistatic situation.

Let us note that all the constitutive laws involve the reactions to the internal constraints when needed, which are clearly non linear relationships, and linear relationships between the forces and the state quantities and velocities. Thus they are simple and we think that they have to account for the main phenomena: non linear constitutive laws are to be chosen only to make the results more adapted but the linear relationships have to be sufficient in a first step to capture the basic physical features. More complicated constitutive law has been considered in [Nedjar 2001; 2002]. For the sake of simplicity, we assume the simplest case of dissipation that is, only the dissipation with respect to the $d\beta/dt$'s and not the dissipation with respect to the gradient of the $d\beta/dt$'s. This assumption minimizes the number of the parameters of the predictive theory, and it is sufficient to ensure both mechanical and mathematical coherency [Bonetti et al. 2006; Bonetti and Schimperna 2004; Bonetti et al. 2005; Frémond and Nedjar 1996].

6. The equations

The principle of virtual power and a proper use of the constitutive laws leads to three sets of equations of motion; the first one is the classical equation of motion and the others are nonstandard partial differential equations describing domains and interface damage evolution.

6.1. *In the domains.* The equations of the evolution of damage for the domains obtained by using the constitutive laws and equilibrium equations are

$$\text{div}(\beta_i \{\lambda_i tr\varepsilon_i(\vec{u}_i)\mathbf{1} + 2\mu_i\varepsilon_i(\vec{u}_i)\}) + \vec{f}_i = 0, \tag{11}$$

$$c_i \frac{d\beta_i}{dt} - k_i \Delta\beta_i + \partial I(\beta_i) + \partial I_-\left(\frac{d\beta_i}{dt}\right) \ni w_i - \frac{1}{2}\left\{\lambda_i \, (tr\varepsilon_i)^2 + 2\mu_i \varepsilon_i : \varepsilon_i\right\}, \tag{12}$$

with initial conditions

$$\beta_i(x, 0) = \beta_i^0(x), \quad \text{in } \Omega_i,$$
$$\beta_s(x, 0) = \beta_s^0(x), \quad \text{in } \partial\Omega_1 \cap \partial\Omega_2,$$

and boundary conditions

$$\sigma_i \vec{N}_i = \vec{g}_i, \quad \text{in } \partial\Omega_i \backslash (\partial\Omega_1 \cap \partial\Omega_2),$$
$$k_i \frac{\partial\beta_i}{\partial N_i} = 0, \quad \text{in } \partial\Omega_i \backslash (\partial\Omega_1 \cap \partial\Omega_2),$$

where the $\vec{f}_i$ and $\vec{g}_i$ are the exterior body forces and surface traction.

The elements $\partial I(\beta_i)$ and $\partial I_-(\partial\beta_i / \partial t)$ contain reactions which forces β_i to remain between 0 and 1 and $\partial\beta_i / \partial t$ to be negative, to account for the irreversibility of damage. The source of damage in the right-hand side of (12) is a deformation energy that well agrees with experimental results. This model is sufficient to describe the damage phenomena during multi-axial loading and unloading without changing the sign of exterior actions. In case the exterior actions change sign, a slightly more sophisticated theory is to be used following [Frémond and Nedjar 1996; Frémond 2001]. It involves the positive and negative parts of the deformations. The positive and negative part of a tensor are obtained after diagonalization (see [Frémond and Nedjar 1996] for details), implying the evaluation of the principal deformations. This is a linear algebra result which holds for symmetric matrices. In particular, considering the positive (or negative) part of the strain tensor leads to an elastic-damage model that exhibits dissymmetric behaviors between tension and compression. The threshold of damage in compression is greater than the one in tension due to a different source term in Equation (12) (see [Frémond and Nedjar 1996]).

6.2. *On the contact surface.* With the previous constitutive laws, the damage evolution law for the cohesive interface reads, [Freddi and Frémond 2005]

$$c_s \frac{d\beta_s}{dt} - k_s \Delta_s \beta_s + \partial I(\beta_s) + \partial I_-\left(\frac{d\beta_s}{dt}\right) \ni w_s - \frac{\hat{k}_s}{2}(\vec{u}_2 - \vec{u}_1)^2 - k_{s,1}(\beta_s - \beta_1) - k_{s,2}(\beta_s - \beta_2)$$
$$- \int_{\partial\Omega_1 \cap \partial\Omega_2} \frac{k_{s,1,2}}{2}(g^2(\vec{x}, \vec{y}) + g^2(\vec{y}, \vec{x}))\beta_s(\vec{y}) \exp\left(-\frac{|\vec{x} - \vec{y}|^2}{d^2}\right)d\Gamma(\vec{y}), \tag{13}$$

where Δ_s is the surface Laplace operator. The last term is not 0 when $\vec{u}_2 = \vec{u}_1$, and is responsible for the damage resulting from elongation. The glue damage source in the right hand side results from the gap between the two solids, from the elongation (the nonlocal effect) and from the flux of damaging work coming from the concrete. This flux is proportional to the difference of damage between the concrete and the glue (see Figure 1). Thus it is more difficult to damage the glue when the concrete is not damaged. In this case, Equation (13) may be interpreted with a glue threshold equal to $w_s + k_{s,1} + k_{s,2}$, whereas it is w_s when the concrete is completely damaged. Indeed, in some experiments intended to separate two adhering pieces, damage of the pieces is produced to facilitate surface damage. The contact boundary
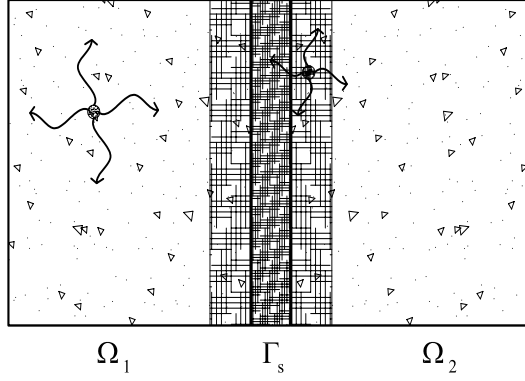
Figure 1. Local interaction between the damage at a material point on the damage on its neighborhood (arrows in the domain), and the damage interaction between domain and interface (arrows in the interphase).

conditions on the glued contact surface $\partial\Omega_1 \cap \partial\Omega_2$ are

$$\sigma_1 \vec{N}_1(\vec{x}) \in \beta_s \hat{k}_s(\vec{u}_2 - \vec{u}_1) + \partial I_-((\vec{u}_2 - \vec{u}_1) \cdot \vec{N}_2)\vec{N}_2$$
$$- \int_{\partial\Omega_1 \cap \partial\Omega_2} 2(\vec{x} - \vec{y})k_{s,1,2} g(\vec{x}, \vec{y})\big(\beta_s(\vec{x})\beta_s(\vec{y})\big) \exp\Big(-\frac{|\vec{x} - \vec{y}|^2}{d^2}\Big) d\Gamma(\vec{y}) \quad (14)$$

for $\vec{x} \in \partial\Omega_1 \cap \partial\Omega_2$,

$$\sigma_2 \vec{N}_2(\vec{y}) \in -\beta_s \hat{k}_s(\vec{u}_2 - \vec{u}_1) - \partial I_-\big((\vec{u}_2 - \vec{u}_1) \cdot \vec{N}_2\big)\vec{N}_2$$
$$- \int_{\partial\Omega_1 \cap \partial\Omega_2} 2(\vec{y} - \vec{x})k_{s,1,2} g(\vec{x}, \vec{y})(\beta_s(\vec{x})\beta_s(\vec{y})) \exp\Big(-\frac{|\vec{x} - \vec{y}|^2}{d^2}\Big) d\Gamma(\vec{x}) \quad (15)$$

for $\vec{y} \in \partial\Omega_1 \cap \partial\Omega_2$,

$$k_1 \frac{\partial\beta_1}{\partial N_1} = k_{s,1}(\beta_s - \beta_1), \qquad k_2 \frac{\partial\beta_2}{\partial N_2} = k_{s,2}(\beta_s - \beta_2), \qquad k_s \frac{\partial\beta_s}{\partial N_s} = 0 \in \partial\big(\partial\Omega_1 \cap \partial\Omega_2\big). \quad (16)$$

For the sake of simplicity, we neglect in the numerical simulations the nonlocal mechanical effect in surface stresses (14) and (15) because it is negligible compared to the local effect. The values of parameters $\hat{k}_s \gg k_{s,1,2}$ of the constitutive laws we choose in the sequel agree with this assumption (see Table 1). Thus the stress on the interface Γ_s becomes the sum of the reaction to the noninterpenetration condition $(\vec{u}_2 - \vec{u}_1) \cdot \vec{N}_2 \leq 0$ and of the elastic interaction $\beta_s \hat{k}_s (\vec{u}_2 - \vec{u}_1)$, with rigidity proportional to β_s, the fraction of undamaged bonds between the two solids.

Boundary condition (16) means that the damaging energy flux in the concrete is proportional to the difference of damage between the glue and the concrete. Parameter $k_{s,i}$ quantifies the importance of the interaction of the volume and surface damages. When $k_{s,1} = 0$ there is no influence of the volume damage on the surface damage. The damage equations are uncoupled and the interface acts as a damage barrier (see the four point bending test in Section 7).

L (mm)	400
l (mm)	300
h (mm)	50
d (mm)	100
t (mm)	100
E (MPa)	38000
ν	0.2
c (MPa· s)	2×10^{-3}
k (mm)	0.3
w (MPa)	2×10^{-5}
$P_{\max}^{\text{one}}$ (kN)	14.3
$P_{\max}^{\text{two}}$ (kN)	18.2

$\hat{k}_s^{\parallel}$ (MPa · mm^{-1})	1.9×10^3
$\hat{k}_s^{\perp}$ (MPa · mm^{-1})	1.9×10^3
c_s (MPa · mm· s)	7.2×10^{-2}
k_s (MPa · mm^2)	0.1
w_s (MPa · mm)	1.1×10^{-2}
$k_{s,1}$ (MPa · mm)	0.1
$k_{s,2}$ (MPa · mm)	0.1
d (mm)	10
$k_{s,1,2}$ (MPa/mm)	20

Table 1. Left: Geometrical, mechanical parameters of the two concrete pieces and maximum loads for four-point bending tests of Figure 2. Right: Glue parameters for the same tests.

In the classical interface problem (that is, one without damaging materials) it is possible to obtain a bilateral connection simply by imposing $\hat{k}_s \cong \infty$. However, in the case we consider — the damaging phenomena of the two materials — a perfect interface is obtained by imposing not only $\hat{k}_s \cong \infty$ but also $k_{s,1} \cong \infty$ and $c_s = w_s = k_s \cong 0$, in order to have the continuity of damage and of its flux across the interface.

As a test to underline the physical meaning of the damage interaction parameters, we consider two square pieces of concrete $[0, 0.05\, m]^2$ connected by a cohesive interface in a pure traction test, that is, where opposite vertical tractions are applied along the horizontal sides of the two bodies. We suppose that the interface is very strong such that no damage appears along the contact surface. Normally, with the two bodies subjected to nearly uniform traction, a diffused damage should involve the whole domains.
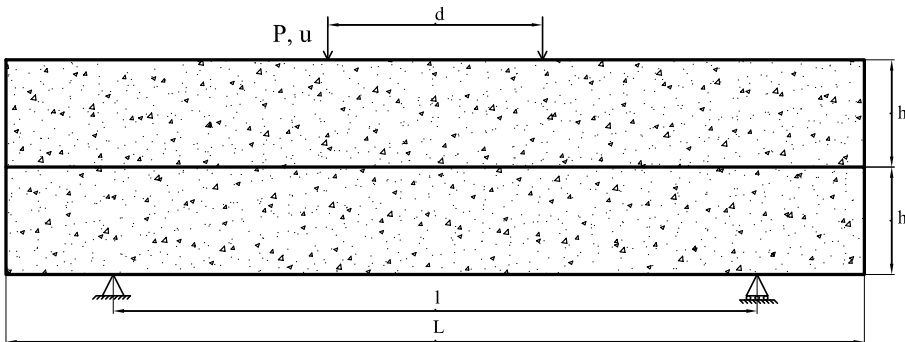
Figure 2. Four point bending test for sample of thickness t. See Table 1 for parameter values for numerical and experimental results.
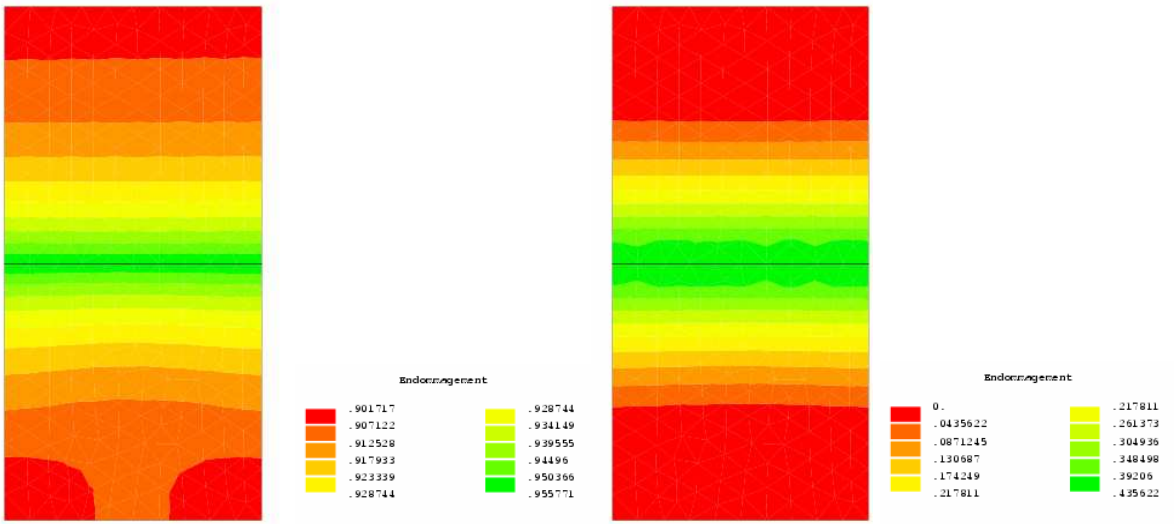
Figure 3. Damage evolution in pure-traction test: $k_{s,1} = k_{s,2} = 0.05$. Note the (green) less damaged zone due to the strong glue connecting the two specimen. The left figure represents an initial damaged state while the right figure shows the complete damaged state. The glue acts as a reinforcement for the material.
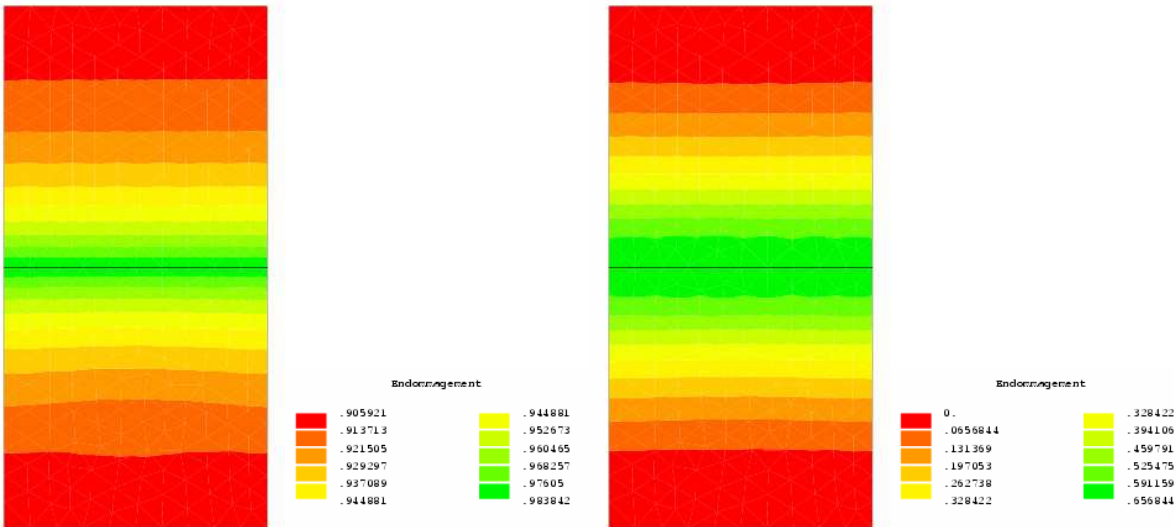
Figure 4. Damage evolution in pure-traction test: $k_{s,1} = k_{s,2} = 0.2$. The left figure represents an initial damaged state while the right figure shows the complete damaged state. The (green) less damaged zone is more important when the interaction parameters $k_{s,i}$ are large. The glue acts like a reinforcement for the material, but is stronger than the case shown in Figure 3.

Instead, as shown in the Figures 3 and 4, the interaction between the glue and the materials determines the presence of more resistant zones next to the interface. Particularly, the zone is larger and the phenomenon more pronounced for higher $k_{s,1}$ and $k_{s,2}$ values.

In view of the examples and experiments investigated in the sequel, we define three models which differ by their surface properties:

- Model a: uncoupled without elongation effects where $k_{s,1} = 0$, $k_{s,2} = 0$, $k_{s,1,2} = 0$;
- Model b: coupled without elongation effects where $k_{s,1,2} = 0$;
- Model c: coupled with elongation effects, that is, the complete model with every physical action.

All other quantities are not zero in any of the models.

7. Numerical simulations and some experimental results

The proposed model has been implemented in the finite element code CESAR-LCPC, [Humbert et al. 2005]. The coupled damage-mechanics model is solved in a semicoupled fashion. Given a time increment, the motion equation (11) is solved first assuming that the damage variables are constants. This equation is solved with a quasi-Newton method. Moreover, in order to deal with the unilateral boundary conditions an ad hoc Uzawa algorithm has been implemented. Afterwards, the damage equations (12) and (13) are solved via a Cranck-Nicholson scheme, and boundary conditions (16) are included explicitly.

Actually, mathematical results concerning the existence of the solution, the proof that the problem is well posed, and numerical verification will appear in a forthcoming paper [Bonetti et al. 2006].

In the following simulations the loads applied are always monotonic and do not change in sign. In particular, all the analysis have been carried out under displacement control. An explicit linear relationship between the time and the imposed displacement is introduced. Moreover, plain strain hypothesis is assumed. Finally, the interface stiffness matrix $\hat{k}_s$ is composed by normal $\hat{k}_s^{\perp}$ and tangential component $\hat{k}_s^{\parallel}$ with respect to the surface orientation. It should be mentioned that the damage scale in each iso-value picture is always represented by green-to-red variation, but it is representative of different damage values and the deformation scale for horizontal and vertical displacement is adapted to numerical results.

7.1. *Four-point bending test.* The goal of this analysis is to validate the model and to evaluate the influence of the enhancements to it that we introduced: the coupling between the damage in the domains and the damage in the interface and the nonlocal elongation contribution to interface damage evolution. In particular, this test shows the importance of the interaction parameters $k_{s,1}$ and $k_{s,2}$ which couple the damages of solids 1 and 2. When solid 1 becomes damaged in the neighborhood of solid 2, solid 2 also becomes damaged. Also the test shows that it is more difficult to damage the glue when the concrete is not damaged than when the concrete is damaged. As already noted, the glue cohesion or threshold is $w_s + k_{s,1} + k_{s,2}$ when the concrete is not damaged whereas it is w_s when concrete is completely damaged in the two solids.

7.1.1. *Test setup and experimental results.* Figure 2 on page 1218 shows a classical four-point bending test. Experimental tests performed by Thaveau [2005] have been considered. We used two different test configurations: one concrete specimen, and two concrete specimens connected with via epoxy glue. The maximum loads obtained, the geometrical and mechanical properties of the specimens are reported in
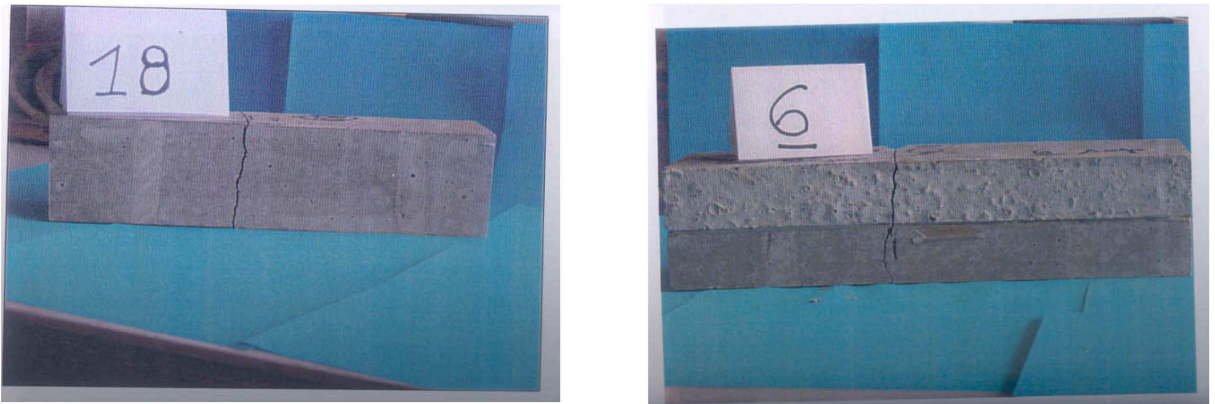
Figure 5. Experimental tests: one specimen on the left; two glued specimens on the right [Thaveau 2005].

Table 1. It should be noted that the maximum load is greater for the glued concrete specimen. Figure 5 show clearly the failure mechanism for the two configurations. In both cases, a vertical fracture in the middle of the specimens appears which propagates from the bottom to the upper face of the beam.

7.1.2. *Numerical results.* The load versus displacement curves obtained from the numerical simulations for single and double specimens are shown in Figure 6. In particular, the case of the uncoupled model
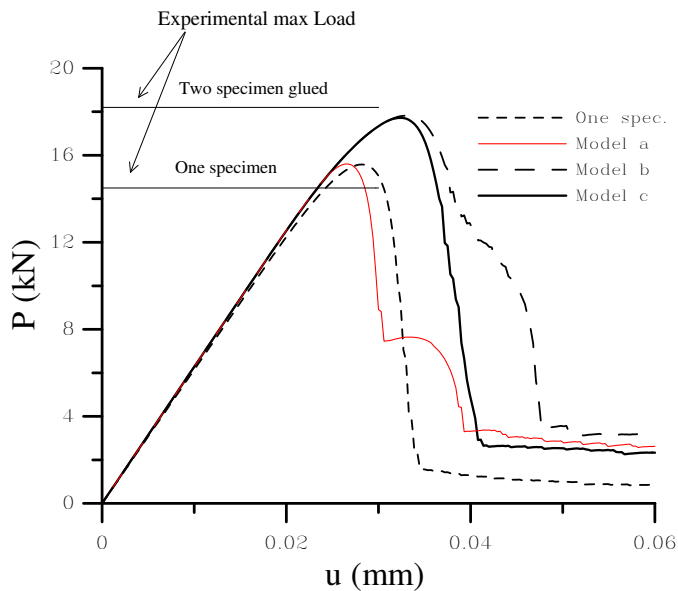
Figure 6. Load versus displacement curves for single and double glued specimens in four point bending tests. The short dashed line is the curve for one specimen, while the red line, the long dashed line, and the straight line are the load versus displacement curves for two glued pieces of concrete obtained with models a, b and c, respectively.
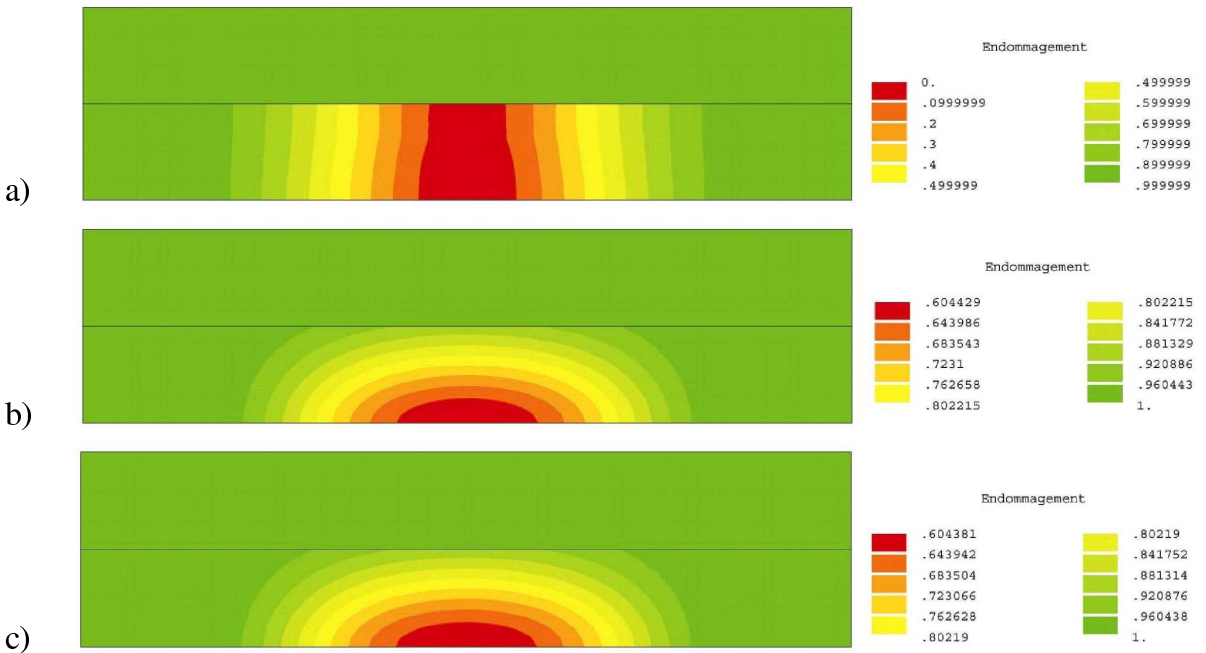
Figure 7. Four point bending test. Damage field at displacement $u = 0.03$ mm for model a (uncoupled damage without elongation effect), model b (coupled damage model for concrete and glue without elongation effect), and model c (coupled 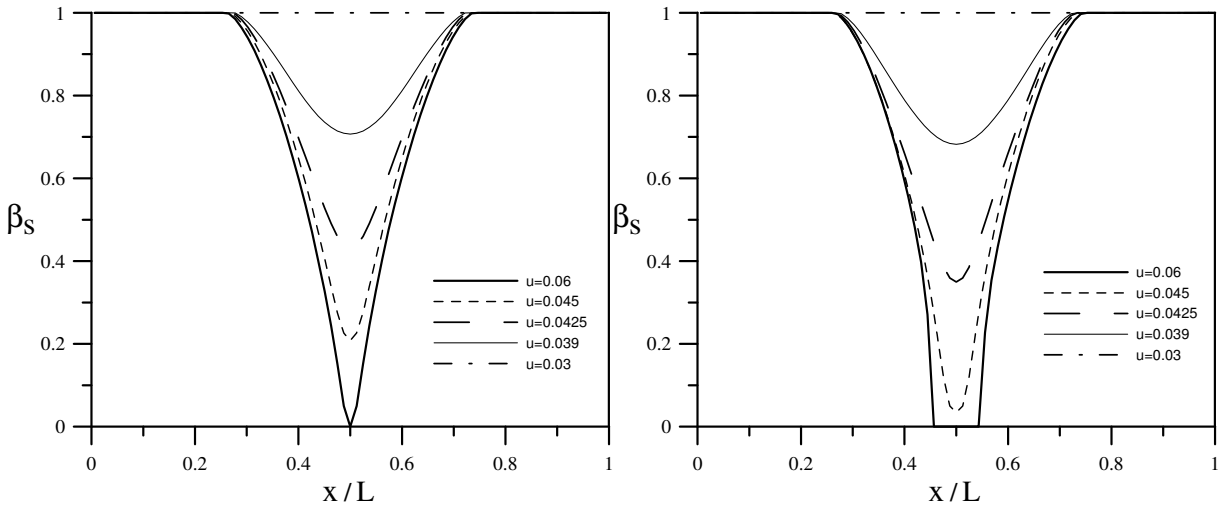damage model for concrete and glue with elongation effect). At the beginning, the contact surface acts as a damage barrier.

presents a very strange hill in the softening branch. This unrealistic behavior completely vanishes when we consider model c with both enhancements, and it is less pronounced in the coupled model b where the nonlocal elongation effect is neglected. The horizontal paths in load versus displacement curves represent structural effects and interplay between surface and volume damage. A similar effect is exhibited in experiments [Gonzalez et al. 2005]. Moreover, for large displacement values the hypothesis of small deformation is no longer sufficient fully to completely describe the failure phenomena [Nedjar 2002].

The damage fields of the two concrete domains for the damage models uncoupled (model a), coupled (model b) and coupled with the nonlocal elongation contribution (model c) are shown in Figures 7–8 for different displacement values: 0.03, 0.045, 0.06 mm. These figures clearly show the inability of the uncoupled model to describe correctly the physical failure phenomenon. In fact, the interface acts as a barrier to the damage propagation, causing the entire damaging of the inferior specimen. On the contrary, the coupling between damages allows correct description of the damage evolution inside the domains. Additional comments are reported in captions. The interface damage evolutions for models b and c are reported in Figure 9.

For model b, the damage of the interface is almost incomplete (that is, $\beta_s \neq 0$) even if the fracture has already crossed the glue thickness. To capture the correct behavior, in the coupled model it is necessary to introduce also the nonlocal elongation contribution. In this test, model a presents no glue damage at
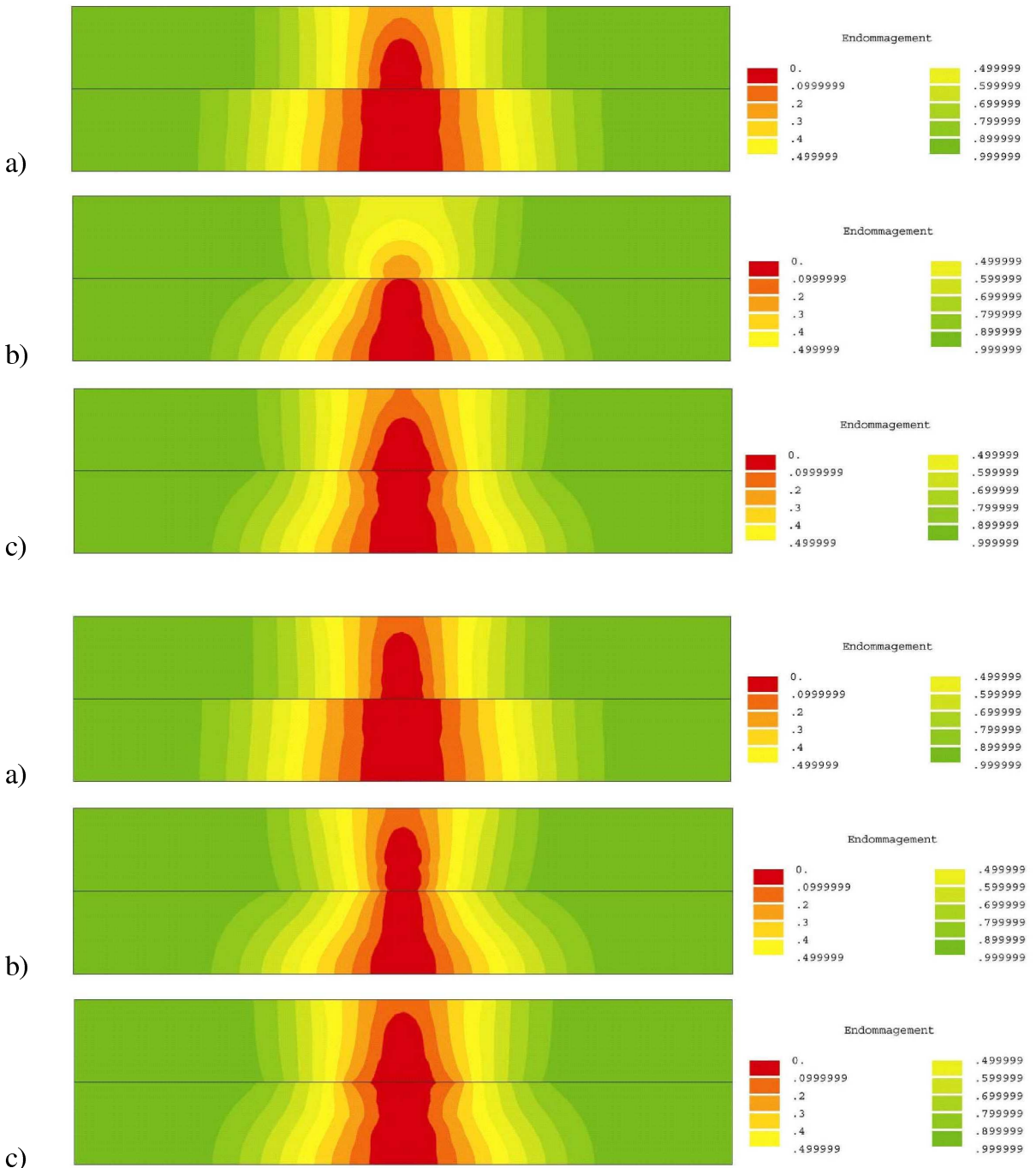
Figure 8. Four point bending test. Damage field at displacement $u = 0.045$ mm (top) and $u = 0.06$ mm (bottom) for model a (uncoupled damage without elongation effect), model b (coupled damage model for concrete and glue without elongation effect), and model c (coupled damage model for concrete and glue with elongation effect).

Figure 9. Four point bending test. Left: Surface damage field β_s along the interface for model b (coupled damage model for concrete and glue without elongation). Right: Surface damage field β_s along the interface for model c (coupled damage model for concrete and glue with elongation). The effect of the elongation is to enlarge the damage zone of the glue, which is completely broken in the middle of the specimen.
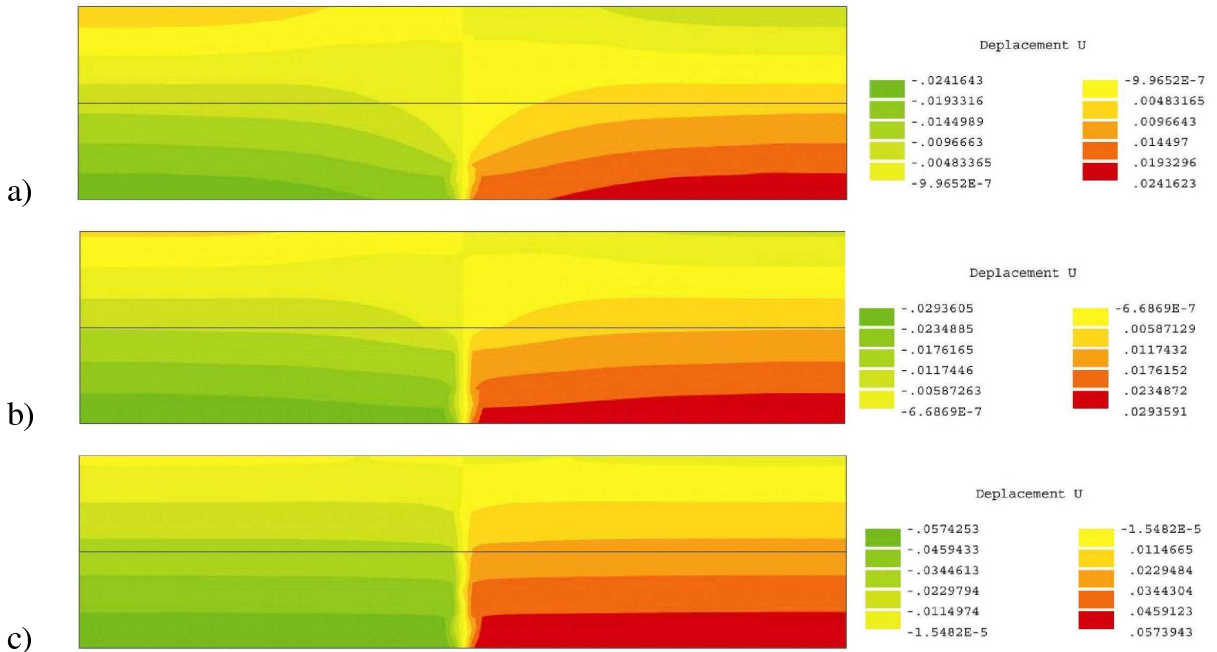
Figure 10. Four point bending test. Horizontal displacement field evaluated at different equilibrium points ($\bar{u} = 0.03, 0.045, 0.06$ mm) for model c. The displacement discontinuity of the horizontal displacement accounts for the fracture in the middle of the sample (see experimental results of Figure 5).
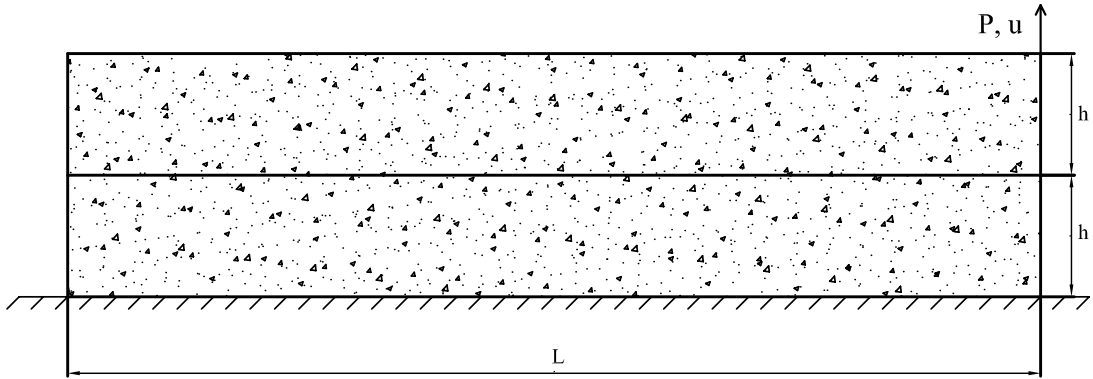
Figure 11. Pull test. The load P is applied on the right and produces displacement u.

L (mm)	400		$\hat{k}_s^{\parallel}$ (MPa· mm^{-1})	$2. \times 10^2$
h (mm)	50		$\hat{k}_s^{\perp}$ (MPa· mm^{-1})	$5. \times 10^2$
E^{up} (MPa)	40000		c_s (MPa· mm· s)	7.2×10^{-3}
E^{dw} (MPa)	35000		k_s (MPa · mm^2)	0.1
ν	0.2		w_s^{strong} (MPa · mm)	10.3×10^{-3}
c (MPa· s)	2×10^{-3}		w_s^{weak} (MPa · mm)	5.15×10^{-3}
k (mm)	0.3		$k_{s,1}$ (MPa · mm)	0.1
w^{up} (MPa)	2×10^{-3}		$k_{s,2}$ (MPa · mm)	0.1
w^{dw} (MPa)	2×10^{-5}		$d(mm)$	5
			$k_{s,1,2}$ (MPa/mm)	10

Table 2. Left: Geometrical, mechanical parameters of the two concrete pieces in Figure 11. Right: Glue parameters for the two pull tests in the same.

all because $\vec{u}_1 - \vec{u}_2 \cong 0$. Horizontal displacement fields are shown in Figure 10 for different values of applied vertical displacement $\bar{u} = 0.03, 0.045, 0.06$ mm. The discontinuity of the displacement clearly shows the fracture propagation in the middle of the specimen.

7.2. *Pull test.* A vertical force is applied to the free right corner of the upper piece of concrete, Figure 11. The relative stiffness of the concrete and of the glue governs the behavior of the structure. The geometrical and mechanical properties of the specimens of two tests are reported in Table 2. If the glue is strong and the concrete is weak, damage occurs in concrete just under the contact surface (Figure 12), in full agreement with experimental results [Theillout 1983]. On the other hand, if the glue is weak and the concrete is solid, separation of the two pieces occurs on the contact surface and the concrete is not damaged (Figure 13). Interface damage evolution is reported in Figure 14. Observe that even if the global structural response for the two simulations is very similar (see Figure 15) the failure mechanisms are completely different.
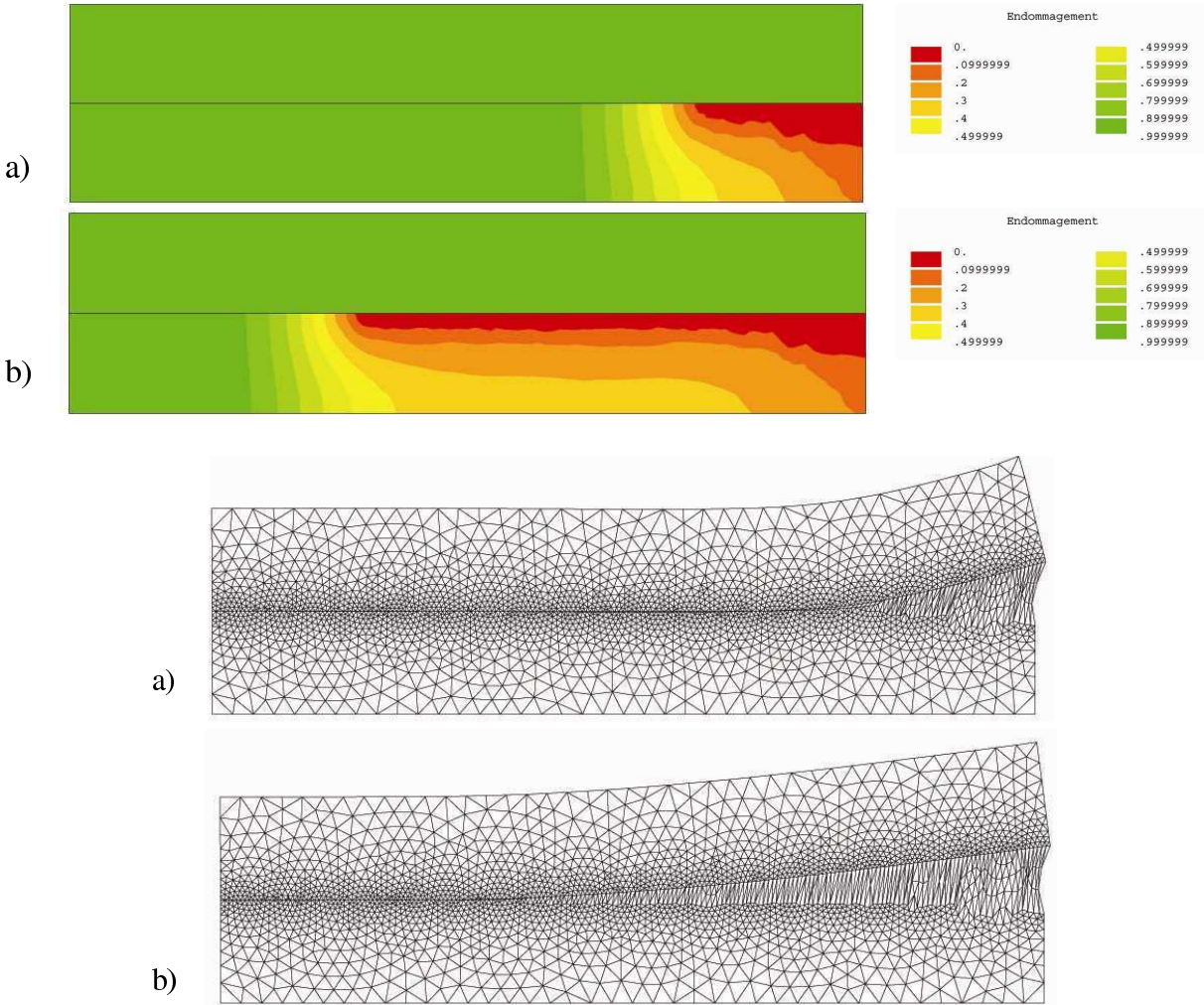
Figure 12. Delamination with strong glue. Top: Damage field at displacement (a) $u = 0.0625$ mm, and (b) $u = 0.3$ mm. A thin damaged zone appears under the interface. Bottom: Deformed configurations at displacement (a) $u = 0.0625$ mm and (b) $u = 0.3$ mm. The concrete breaks just under the contact surface while the glue remains intact. In this simulation no damage appears in the interface, so $\beta_s = 1$.

7.3. *FRP-concrete delamination test.* External bonding of fiber-reinforced polymer (FRP) plates or sheets has recently emerged as a popular method for strengthening reinforced concrete (RC structures). The behavior of such FRP-strengthened RC structures is often controlled by the behavior of the interface between FRP and concrete, which is commonly studied through a pull test in which an FRP sheet or plate is bonded to a concrete prism and is subjected to tension. Figure 16 shows a typical configuration for a pull-pull delamination test, [Point and Sacco 1996]. Left and bottom sides of the specimen have been fixed in order to have no displacements in the direction normal to the surface and free displacements
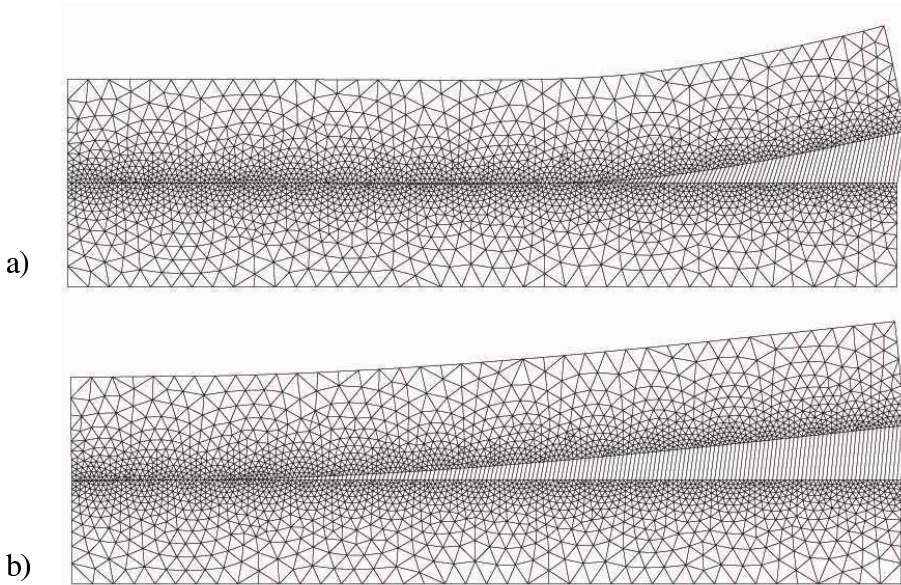
Figure 13. Delamination with weak glue. Top: Deformed configurations at displacement (a) $u = 0.0625$ mm and (b) $u = 0.3$ mm. The glue breaks progressively and there is almost no damage within the concrete. The straight lines connecting the two pieces of concrete represent the gap. $\vec{u}_2 - \vec{u}_1$.

tangent to it. Existing studies reported in [Yao et al. 2005] suggest that the main failure mode of FRP-to-concrete bonded joints in pull tests is concrete failure under shear which occurs generally at a few millimeters from the adhesive layer as shown in Figure 17 (see [Ferracuti et al. 2006]).
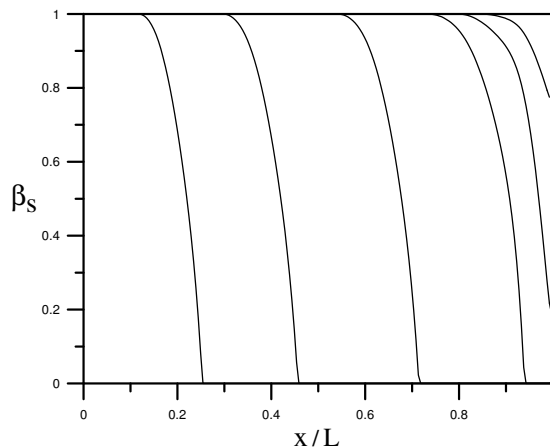
Figure 14. Delamination with weak glue. Damage interface evolution of the glue. The damage field $\beta_s(x/l, t)$ is plotted at different times t.
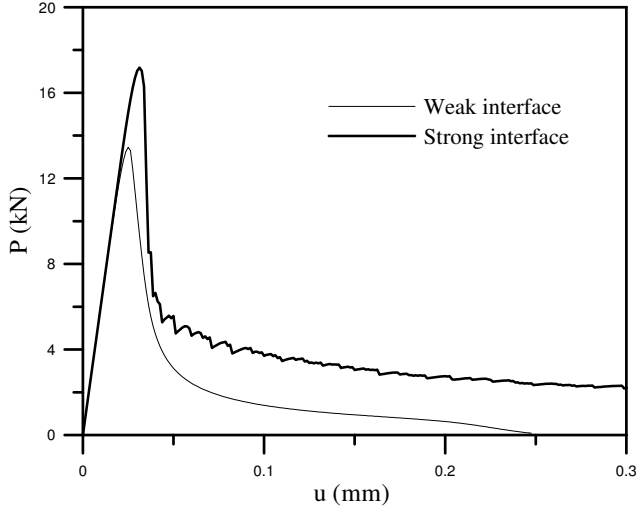
Figure 15. Pull test. Load versus displacement curves obtained for different stiffness values. It is important to observe that even if the global structural response for the two simulations is very similar, the failure mechanisms are completely different, as outlined from the previous Figures 12, 13, and 14.

The geometrical and mechanical properties of the specimens are reported in Table 3. The numerical simulation (Figures 18 and 19) clearly shows a thin damaged zone in the concrete as well as large displacements. The damaged zone corresponds to a small layer of concrete which remains glued on the FRP in the experiments.

L (mm)	100			$\hat{k}_s^{\parallel}$ (MPa· mm^{-1})	$5. \times 10^2$
d(mm)	100			$\hat{k}_s^{\perp}$ (MPa· mm^{-1})	$1. \times 10^3$
h (mm)	50	t (mm)	1.016	c_s (MPa· mm· s)	7.2×10^{-2}
E (MPa)	33640	E (MPa)	230000	k_s (MPa · mm^2)	0.1
ν	0.2	ν	0.3	w_s (MPa · mm)	10.3×10^{-4}
c (MPa· s)	2×10^{-3}	c (MPa· s)	2×10^{-3}	$k_{s,1}$ (MPa · mm)	0.1
k (mm)	0.2	k (mm)	0.1	$k_{s,2}$(MPa · mm)	0.2
w (MPa)	4×10^{-5}	w (MPa)	2×10^{-2}	d (mm)	5
				$k_{s,1,2}$ (MPa/mm)	20

Table 3. Geometrical, mechanical parameters of the concrete for the pull-pull test (left), the FRP (middle), and the FRP-concrete pull-pull test (right).
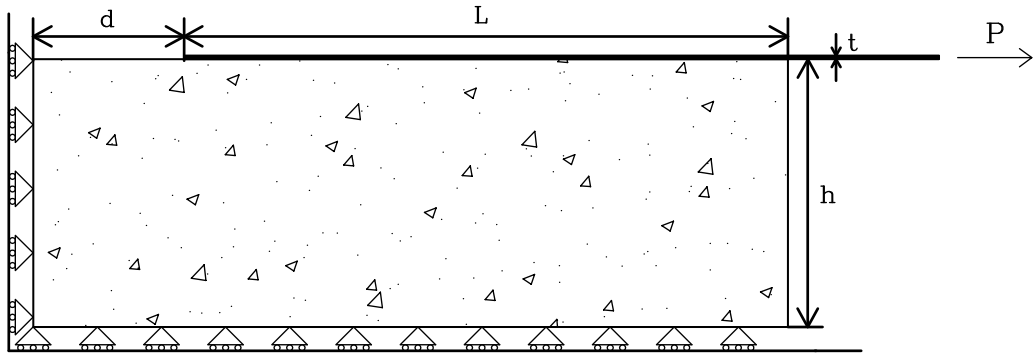
Figure 16. FRP-concrete pull-pull delamination test [Freddi and Savoia 2006].

Figure 17. FRP-concrete pull-pull delamination test: experimental failure mode [Yao et al. 2005].

8. Conclusions

The predictive model which has been derived with the continuum mechanics theory involves only macroscopic quantities. The few parameters of the model can be measured with sample and structure experiments. The numerous results concerning different structures and experiments show the ability of the model to deal with engineering problems and predict failure modes. As outlined in the examples, once the damage is diffused and very low load bearing capacity remains, large displacement values may
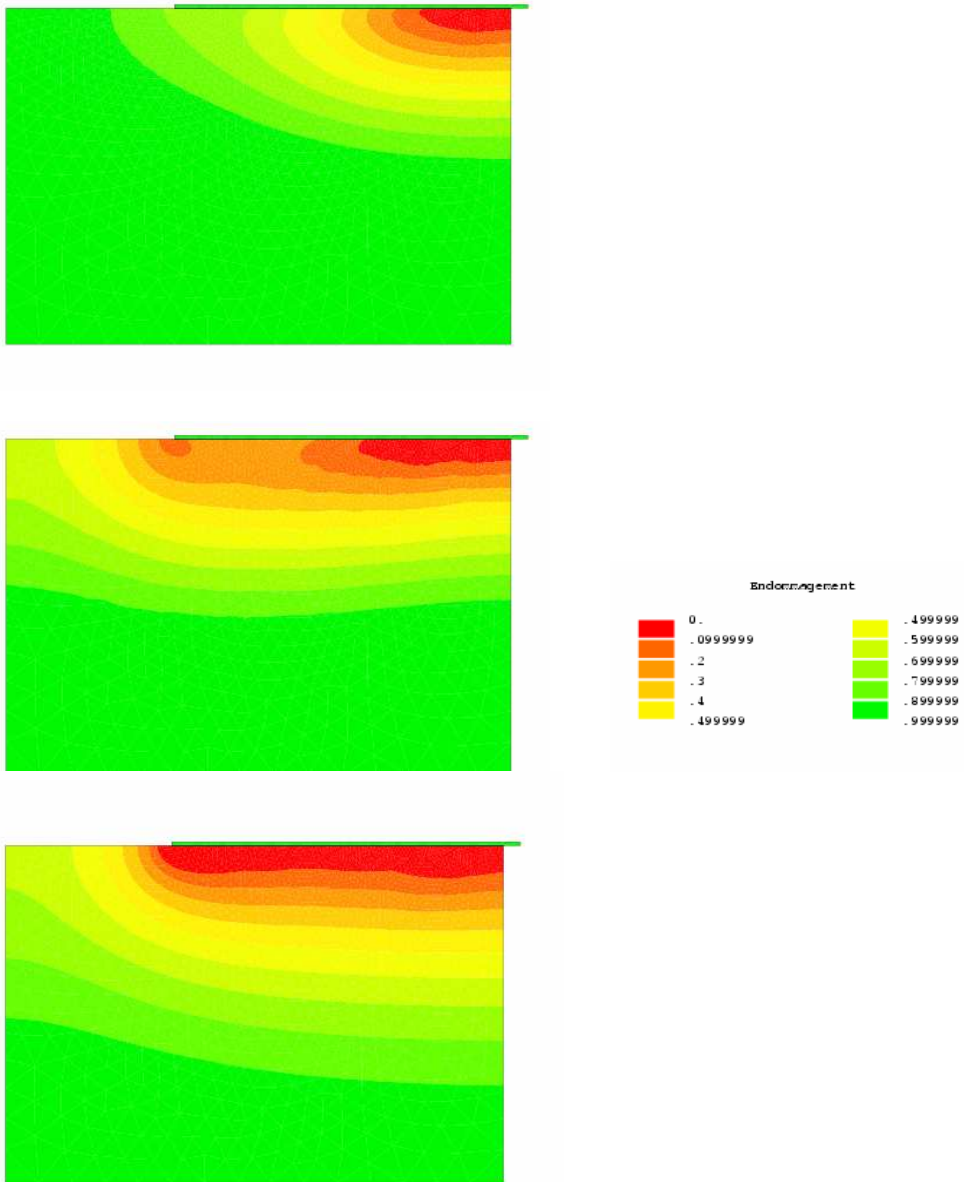
Figure 18. FRP-concrete pull-pull delamination test. Damage evolution. A thin zone is damaged under the reinforcement.

appear such that the hypothesis of small deformations may no longer be sufficient to describe the failure phenomena completely [Nedjar 2002]. In this case, large deformation theory should be considered.

Finally, this model is applicable to the design of concrete structures as well as other composite structures.
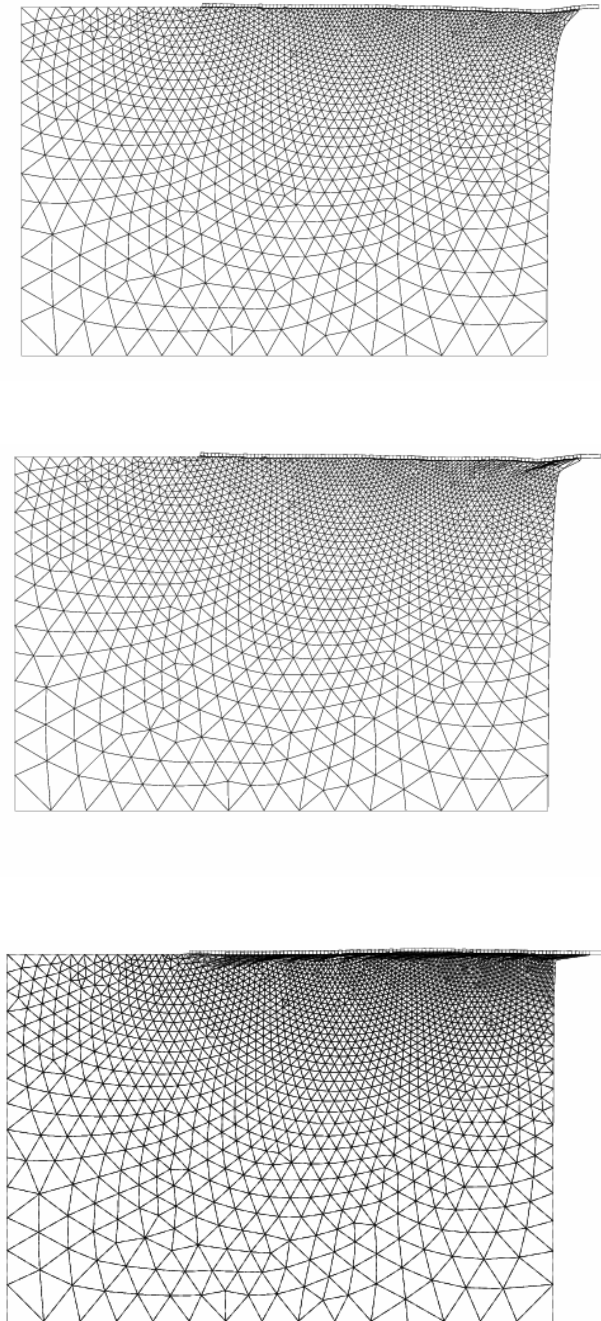
Figure 19. FRP-concrete pull-pull delamination test. Deformed configurations. The thin damaged zone under the reinforcement results in large deformation. The displacement scale is different in each deformed mesh.

References

[Aimi et al. 2007] A. Aimi, M. Diligenti, and F. Freddi, "Numerical aspects in the SGBEM solution of softening cohesive interface problems", *J. Comput. Appl. Math.* (2007). In press.

[Alfano and Crisfield 2001] G. Alfano and M. Crisfield, "Finite element interface models for the delamination analysis of laminated composites: Mechanical and computational issues", *Int. J. Numer. Methods Eng.* **50**:7 (2001), 1701–1736.

[Bonetti and Schimperna 2004] E. Bonetti and G. Schimperna, "Local existence to Fremond's model for damaging in elastic materials", *Continuum Mech. Therm.* **16** (2004), 319–335.

[Bonetti et al. 2005] E. Bonetti, G. Bonfanti, and R. Rossi, "Global existence for a contact problem with adhesion", Preprint 16, Università di Brescia, Italy, 2005, Available at http://www.dmf.unicatt.it/cgi-bin/preprintserv/semmat/Quad2005n16.pdf.

[Bonetti et al. 2006] E. Bonetti, F. Freddi, and M. Frémond, "Coupled volume and surface damage: An existence theory", 2006. Preprint.

[Borino and Failla 2005] G. Borino and B. Failla, "An elastic interface model with nonlocal integral damaging effects", in *Atti del XVII Congresso dell'Associazione Italiana di Meccanica Teorica e Applicata* (Florence), September 2005. Available on CD.

[Bruneaux 2004] M. A. Bruneaux, *Durabilité des assemblages collés: Développement d'un modèle mécanique prédictif avec prise en compte des caractéristiques physico-chimiques de l'adhésif*, Ph.D. thesis, Ecole National des Ponts et Chaussées, Paris, and University Tor Vergata, Rome, 2004.

[Chau et al. 2004] O. Chau, M. Shillor, and M. Sofonea, "Dynamic frictionless contact with adhesion", *Z. Angew. Math. Phys.* **55**:1 (2004), 32–47.

[Ferracuti et al. 2006] B. Ferracuti, M. Savoia, and C. Mazzotti, "A numerical model for FRP-concrete delamination", *Compos. B Eng.* **37**:4–5 (2006), 356–364.

[Freddi and Frémond 2005] F. Freddi and M. Frémond, "A damage model for domains and interfaces problem", in *Atti del XVII Congresso dell'Associazione Italiana di Meccanica Teorica e Applicata* (Florence), September 2005. Available on CD.

[Freddi and Savoia 2006] F. Freddi and M. Savoia, "Analysis of FRP-concrete delamination via boundary integral equations", *Eng. Fract. Mech.* (2006). In press.

[Frémond 2001] M. Frémond, *Non-smooth thermomechanics*, Springer, Heidelberg, 2001.

[Frémond and Nedjar 1996] M. Frémond and B. Nedjar, "Damage, gradient of damage and principle of virtual power", *Int. J. Solids Struct.* **33**:8 (1996), 1083–1103.

[Frémond et al. 1998] M. Frémond, K. L. Klutter, B. Nedjar, and M. Shillor, "One-dimensional damage model", *Adv. Math. Sci. Appl.* **8**:2 (1998), 541–570.

[Gonzalez et al. 2005] D. Gonzalez, K. Benzarti, L. Gonon, and H. De Baynast, "Durability of the concrete epoxy/adhesive bond: Micro- and macro-scale investigations", pp. 413–420 in *Third International Conference on Composites in Construction* (Lyon), edited by P. Hamelin et al., July 2005.

[Humbert et al. 2005] P. Humbert, G. Fezans, A. Dubouchet, and D. Remaud, "CESAR-LCPC, un progiciel de calcul dédié au génie civil", *Bull. Lab. Ponts Chaussées* **256–257** (2005), 7–37.

[Ireman 2005] B. Ireman, "Algorithm for gradient damage models based on semi-smooth Newton method", *Comput. Methods Appl. Mech. Eng.* **194**:6–8 (2005), 727–741.

[Lemaitre 1992] J. Lemaitre, *A course on damage mechanics*, Springer, Berlin, 1992.

[Lemaitre and Desmorat 2005] J. Lemaitre and R. Desmorat, *Engineering damage mechanics: Ductile, creep, fatigue and brittle failures*, Springer, Berlin, 2005.

[Moreau 1966] J. J. Moreau, "Fonctionelles convexes: Séminaire sur les équations aux dérivates partielles", Lecture notes, Collége de France, Paris, 1966. Reprinted Istituto Poligrafico e Zecca dello Stato, University Tor Vergata, Rome 2003.

[Mosconi 2006] M. Mosconi, "Uniqueness and minimum theorems for a multifield model of brittle solids", *Int. J. Solids Struct.* **43**:11–12 (2006), 3428–3443.

[Nedjar 2001] B. Nedjar, "Elastoplastic-damage modelling including the gradient of damage: Formulation and computational aspects", *Int. J. Solids Struct.* **38**:30–31 (2001), 5421–5451.

[Nedjar 2002] B. Nedjar, "A theoretical and computational setting for a geometrically nonlinear gradient damage modelling framework", *Comput. Mech* **30**:1 (2002), 65–80.

[Point and Sacco 1996] N. Point and E. Sacco, "A delamination model for laminated composites", *Int. J. Solids Struct.* **33**:4 (1996), 483–509.

[Raous and Monerie 2002] M. Raous and Y. Monerie, "Unilateral contact, friction and adhesion: 3D cracks in composite materials", pp. 333–343 in *Contact Mechanics: Proceedings of the Third Contact Mechanics International* (Peniche), Kluwer, 2002.

[Raous et al. 1999] M. Raous, L. Cangémi, and M. Cocu, "A consistent model coupling adhesion, friction, and unilateral contact", *Comput. Methods Appl. Mech. Eng.* **177**:3–4 (1999), 383–399.

[Stumpf and Hackl 2003] H. Stumpf and K. Hackl, "Micromechanical concept for the analysis of damage evolution in thermo-viscoelastic and quasi-brittle materials", *Int. J. Solids Struct.* **40**:6 (2003), 1567–1584.

[Thaveau 2005] M. P. Thaveau, "Flexion quatre points de prismes en béton collés", 2005. Laboratoires des Ponts et Chaussées, Internal report.

[Theillout 1983] J. N. Theillout, *Renforcement et réparation des ouvrages d'art par la technique des tôles colléees*, Ph.D. thesis, Ecole National des Ponts et Chaussées, Paris, 1983.

[Truong Dinh Tien 1990] J. M. Truong Dinh Tien, *Contact avec adhérence*, Ph.D. thesis, Université Pierre et Marie Curie, Paris, 1990.

[Voyaiadjis et al. 1998] G. Z. Voyaiadjis, J. J. W. Woody, and J. L. Chaboche, *Damage mechanics in engineering materials*, Elsevier, 1998.

[Yao et al. 2005] J. Yao, J. G. Teng, and J. F. Chen, "Experimental study on FRP-to-concrete bonded joints", *Compos. B Eng.* **36**:2 (2005), 99–113.

[Zou et al. 2003] Z. Zou, S. Reid, and S. Li, "A continuum damage model for delamination in laminated composites", *J. Mech. Phys. Solids* **51**:2 (2003), 333–356.

FRANCESCO FREDDI: francesco.freddi@unipr.it
Department of Civil Engineering & Architecture, University of Parma, Viale Usberti 181/A, 43100 Parma, Italy

MICHEL FRÉMOND: fremond@cmla.ens-cachan.fr
Laboratoire Lagrange, Laboratoire Central des Ponts et Chausées - LCPC, 58 Boulevard Lefebvre, 75732 Paris Cedex 15, France

JOURNAL OF MECHANICS OF MATERIALS AND STRUCTURES

http://www.jomms.org

BOARD OF EDITORS

PRODUCTION

Journal of Mechanics of Materials and Structures

Volume 1, Nº 7   September 2006